Fuzzy Logic-based Maximum Power Point Tracking for a Solar Electric Vehicle

Thameur Obeidi[1,2], Cherif Larbes[2], Adrian Ilinca[1], Gul Filiz Tchoketch Kebir[1,2]

[1]Wind Energy Research Laboratory, Université du Québec à Rimouski, 300, allée des Ursulines, Rimouski, QC, Canada, G5L 3A1, Thameur.Obeidi@uqar.ca, Adrian_Ilinca@uqar.ca, GulFiliz.TchoketchKebir@uqar.ca

[2] Laboratoire des Dispositifs de Communication et de Conversion Photovoltaïque, Département d'Électronique, École Nationale Polytechnique, 10, Avenue Hassen Badi, El Harrach, Alger 16200, Algeria, cherif.larbes@g.enp.edu.dz

Abstract: A maximum power point tracking (MPPT) system, for a very high-efficiency photovoltaic array applied to a solar-powered vehicle, was studied in this work. Photovoltaic energy is a promising alternative energy; however, its high initial cost, it is essential to improve the energy conversion efficiency. Regarding a particular incident solar insolation and temperature, there is a specific voltage at which maximum power may be harvested (Maximum power point, MPP). The Maximum Power Point is therefore achieved at a specific voltage that depends on insolation and temperature. A proper maximum power point tracking system is particularly important for solar-powered vehicles relating to the rapid change of insolation due to the dynamic motion of the vehicle. In this paper, the emphasis is on the potential of energy conversion improvement of a PV system, associated with a moving vehicle via the use of a fuzzy based maximum power point tracking algorithm.

Keywords: Maximum Power Point Tracking (MPPT); the fuzzy controller; Photovoltaic Dynamic Tracking (PVT); solar electric vehicle

1 Introduction

The development of photovoltaic (PV) cells, small and large PV systems has accelerated during recent years. Application of photovoltaic energy has been studied on different systems, namely, satellite power systems, solar power generation, solar battery charging stations, and solar vehicles (cars, ships, and airplanes). Since space, weight, and cost are limiting and defining factors for solar vehicles, it is desirable to harvest maximum energy from installed photovoltaic cells. The present work emphasizes the improvement of power conversion using

state of the art high-performance fuzzy logic based MPPT algorithm. Every photovoltaic cell array has an optimum operating point, called the maximum power point (MPP), which varies depending on cell temperature and incident insolation level. In this paper, a fuzzy controller is used recently in the PV system of a solar vehicle, the performance of this controller is tested and compared to that of a Perturb and Observe (P&O) controller [1, 2, 3, 4] under Matlab-Simulink environment. The other novelty of this controller is the use of a Buck instead of Boost and the use of Gaussian forms instead of Triangular forms in the membership functions.MPPT methods portrayed in the literature [2-29] used different techniques and algorithms which widely differ in performance: convergence speed, implementation complexity, accuracy, and most importantly the cost of implementation of the whole set-up. Regarding to previous study [23, 28], it was presented nineteen different MPPT methods including: "Hill Climbing/P&O method" [5, 7, 19, 21, 25], "Incremental Conductance Method" [6, 8, 21, 26, 27], "Fractional Open-Circuit Voltage Method" [19, 22], "Fractional Short-Circuit Current Method" [21, 22, 25], "Artificial Intelligence-Based MPPT Algorithms" [5, 11, 20, 21, 25], "Current Sweep Method" [5, 20], "DC-Link Capacitor Droop Control method" [5, 20], "Load Current or Load Voltage Maximization method" and "dP/dV or dP/dI Feedback Control technique" [5, 6]. Additional MPPT techniques have been studied as "Linearized I-V Characteristics Method" [8], "Ripple Correlation Control Method" [5, 21, 22], "Current Compensation Method", "Constant Voltage and Current Method", "Parasitic Capacitance Method" [5, 8, 21], "Sliding Mode Control MPPT Technique", "Curve-Fitting Method", "Forced Oscillation Technique"[5, 12], "Particle-Swarm-Optimisation-Based MPPT" [5, 21] and "Hybrid Methods" [5, 6, 13].

MPPT methods have also been applied to solar vehicles. A new Maximum Power Point Tracking (MPPT) control algorithm based on the Incremental Conductance (IncCond) has been applied for a single high-performance gas-solar cell for hybrid and electric vehicle applications [6, 14, 32, 33]. This work concluded that the proposed MPPT algorithm secures a 1.5ms response time under rapid insolation changes. The application of an improved perturbation control method to a Solar Autonomous Underwater Vehicle (SAUV) has been studied in [15, 16, 17, 34, 35]. Particular attention is paid to the equalization charging control method based on an improved P&O controller on a series of Lithium-Ion battery strings. Another study [36, 37] illustrated the efficiency of a maximum power point tracker for compound curve photovoltaic arrays applied to solar-powered vehicles. The article presented an open loop algorithm aiming at maximum power point tracking and use of synchronous rectification in a boost converter to improve the overall circuit efficiency. The application of a modified quadratic maximization MPPT algorithm to a moving vehicle has been studied in [30, 31, 38, 39, 40] together with its performance validation using the Sandia dynamic test protocol. It concluded that the traditional P&O method has a slow restart tracking of the maximum power. It resulted from the literature review that a diversity of MPPT algorithms has been developed for the improvement of energy conversion. Its performances

(convergence speed, implementation complexity, accuracy, and cost of implementation) are variable and subject to improvement. The paper is organized as follows: regarding the second section, we have studied the specificities of PV fields mounted on solar vehicles. The third section is devoted to the energy production chain from the solar panels and up to battery via the DC-DC converter which houses the controller programmed to track the MPP (MPPT) where the study will focus on the comparison of two algorithms. The classic P&O and the FL algorithm proposed to improve the performance of the controller (MPPT); section four comes with the simulation parameters to concretize the simulation of the two models studied in the previous section; the results are discussed in the fifth section.

2 Specificity of Photovoltaic Arrays in a Solar Electric Vehicle

A typical simple configuration of a solar electric vehicle (EV) is shown in Figure 1 [6, 11]. The outputs of individual PV panels are combined and connected to a common DC/DC converter linked to the battery pack. The DC bus voltage is then converted to AC voltage through an inverter to control the machine traction.

However, most solar panels on solar-powered electric vehicles are curved to fold into the aerodynamic shape of the vehicle such that all PV arrays require an MPPT controller for best conversion efficiency. Figure 2 schematizes the different arrays. The MPPT algorithm applies differently to arrays as they are submitted to different incident irradiance and temperature at the same time. Therefore, the imposed voltage for each array is different in order to extract maximum output power.

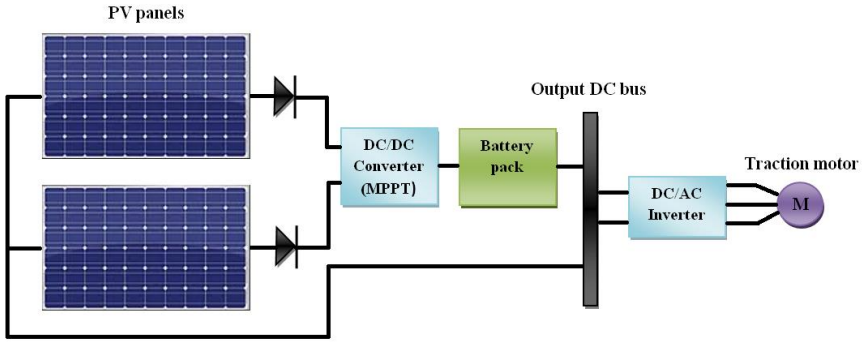

Figure 1
Simple block diagram representation of a solar electric vehicle [11]

3 Elements of Solar Vehicle Power System

A typical solar vehicle power system consists of an array made up of a given number of serially connected photovoltaic cells [1, 6, 7], a parallel-connected battery pack acting as an energy buffer and a DC-DC converter to match the voltage of the solar array with the one of the batteries (Figure 2). The conversion ratio of the converter is varied by a controller to constantly adjust the operating voltage of the solar panel to its point of maximum power (MPP), it is being operated as a Maximum Power Point Tracker (MPPT).

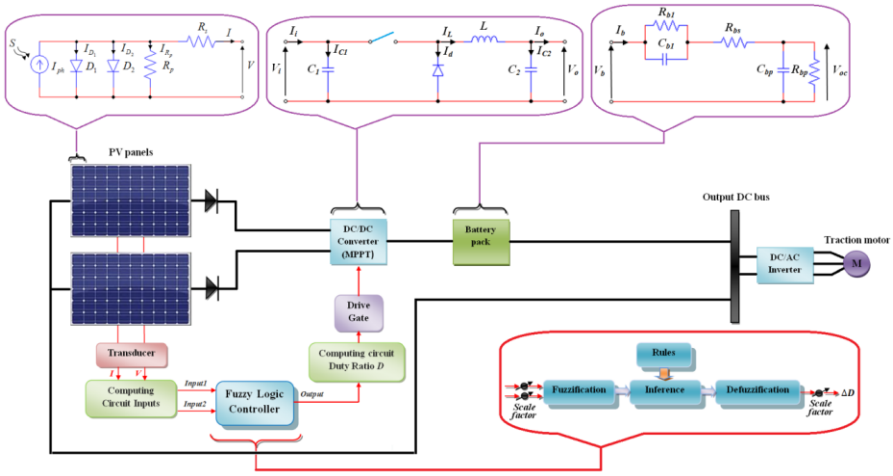

Figure 2
MPPT component architecture for Solar Electric Vehicle with Fuzzy Controller

3.1 Solar Arrays

The photovoltaic (PV) cell model used contains two diodes [14, 18, 29] and is based on the general equation (1). The complete photovoltaic module consists of z photovoltaic cells connected in series:

$$I = S.I_{ph}(T) - I_{s1}\left[e^{\frac{q(V+IzR_s)}{zn_1kT}} - 1\right] - I_{s2}\left[e^{\frac{q(V+IzR_s)}{zn_2kT}} - 1\right] - \frac{V + IzR_s}{zR_p} \quad (1)$$

Where:

$$I_{ph}(T) = I_{ph}\big|_{(T=298K)}\left[1 + (T - 298)\cdot(5\cdot 10^{-4})\right] \quad (2)$$

$$I_{s_1} = K_1 T^3 e^{-\frac{E_g}{kT}} \quad (3)$$

$$I_{s_2} = K_2 T^{\frac{5}{2}} e^{-\frac{E_g}{kT}} \tag{4}$$

In equations (1-4), I and V are respectively the output current and output voltage of the photovoltaic cell, S is the irradiance and T is the absolute temperature in Kelvin. $I_{ph}(T)$ is the generated photo-current, I_{s_1} and I_{s_2} are the diodes reverse saturation currents, n_1 and n_2 the diode ideality factors, R_s the series resistance and R_p the parallel resistance. E_g is the band-gap energy of the semiconductor, q is the elementary charge constant $(1.602 \cdot 10^{-19}\text{C})$, $K_1 = 1.2\ A/cm^2K^3$, $K_2 = 2.9 \times 10^5\ A/cm^2K^{5/2}$ and k the Boltzman constant $(1.38 \times 10^{-23}\text{J/K})$.

3.2 Principle and Motivation for MPPT

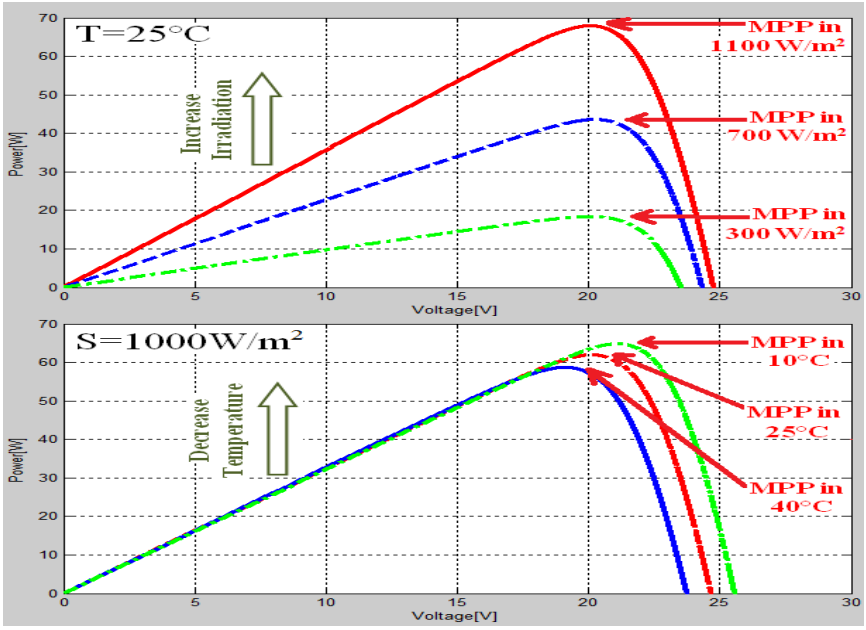

Figure 3
Variation of MPP with changing irradiance and temperature

As illustrated in Figure 3, the harnessed power from photovoltaic arrays, P, does not only depend on its operating voltage V (and load value), but also on incident temperature and irradiance. The point of maximum power indicated as MPP (Maximum Power Point) is the desired operating point for a photovoltaic array to obtain maximum efficiency. In these circumstances, a maximum power point tracking (MPPT) mechanism can help to significantly increase the power output of

a solar power system by adjusting the system parameters (like load or operating voltage V) in such a way that the operating voltage V will always be approximately equal to the optimum operating voltage V_{MPP}. In the case of solar-powered electric vehicles, the use of MPPT is of high importance as it gives an opportunity to boost power and efficiency, despite rapidly varying incident parameters (irradiance and temperature) due to vehicle mobility and aerodynamically curved solar arrays. MPPT helps in securing high power availability without the need for solar panel oversizing in which case, vehicle weight is unnecessarily increased and overall performance diminished [2, 32].

3.3 DC-DC Converter

Photovoltaic systems are generally connected to static converters (DC-DC) driven by preprogramed controllers to continuously analyze the output of the solar panel. MPPT controllers continuously analyze instantaneous power output and adjust the parameters with an aim to maximum energy whatever are the load and atmospheric conditions [16, 20, 32]. In this work, the MPPT device consists of a buck converter between the PV module and the load (Figure 2). Mathematical equations modeling the buck converter are as follows:

$$\frac{V_o}{V_i} = D \tag{5}$$

$$I_o = I_L - C_2 \frac{dV_o}{dt} \tag{6}$$

$$I_L = \frac{1}{D}\left(I_i - C_1 \frac{dV_i}{dt} \right) \tag{7}$$

$$V_i = \frac{1}{D}\left(V_o + L \frac{dI_L}{dt} \right) \tag{8}$$

It is understood from equation (5) and from Figure 4 below, that an increase in conversion duty ratio results in an increase in the output voltage of the buck converter and vice-versa [16, 21, 33, 44].

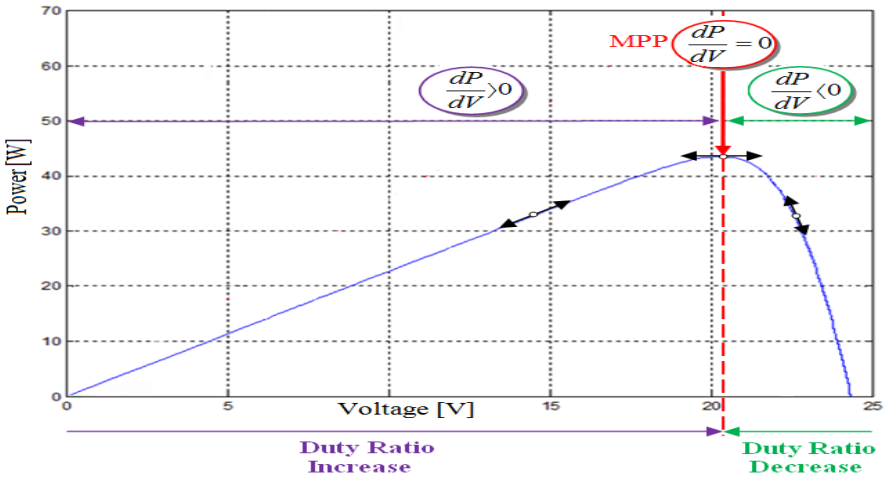

Figure 4
Direction change of the duty ratio D of the buck converter for tracking the MPP

3.4 Solar Vehicle Lead-Acid Batteries

In a photovoltaic power supply system for a car, batteries are used as an energy buffer due to the variability of solar array production and power demand from the vehicle. Using the batteries to store the electrical power from the solar panels in the form of chemical energy makes the generated energy readily available whenever it is needed, independent of the current weather conditions. An equivalent electrical circuit model for the batteries has been established to analyze the dynamic performance and the steady-state behaviour of the whole power system. We use an equivalent electrical circuit model as shown in Figure 2 that includes equivalent components for all major operating characteristics of a lead-acid battery. The representation in Figure 2 illustrates the characteristics of a lead-acid battery in a comprehensive yet very simplified way. Reference [39, 40] proposes additional mathematical expressions used to adjust the model's components to represent the variation with temperature of the battery's characteristics. They do not account for other parameters such as the state of the charge or the electrolyte level, which are additional factors influencing the battery's characteristics. The component values of the battery were modeled in the literature [16, 43, 44, 45], to realize an approximate overvoltage of 27 V at the maximum charging current of 9.5 A. Knopf [29] uses a battery pack consisting of a series of 9 independent 12 V GNB batteries with a specified capacity of 45 Ah each. This adds up to a theoretical operating voltage of 108 V. The actual operating range (V_{min}; V_{max}) of the batteries lies between 90 V and 125 V. The lead-acid battery model can be mathematically expressed in the frequency domain representing the equivalent input impedance of a lead-acid battery:

$$Z(s) = \frac{V_b}{I_b} = R_{bs} + \frac{R_{b1}}{R_{b1}C_{b1}s + 1} + \frac{R_{bp}}{R_{bp}C_{bp}s + 1} \tag{9}$$

The form of equation (9) can be written as:

$$Z(s) = \frac{a_2 s^2 + a_1 s + a_0}{b_2 s^2 + b_1 s + b_0}$$

$$\begin{cases} a_2 = R_{bs}R_{b1}R_{bp}C_{b1}C_{bp} \\ a_1 = R_{bs}R_{b1}C_{b1} + R_{bs}R_{bp}C_{bp} + R_{b1}R_{bp}c_{bp} + R_{bp}R_{b1}C_{b1} \\ a_0 = R_{bs} + R_{b1} + R_{bp} \\ b_2 = R_{b1}R_{bp}C_{b1}C_{bp} \\ b_1 = R_{b1}C_{b1} + R_{bp}C_{bp} \\ b_0 = 1 \end{cases} \tag{10}$$

Equation (9) and parametric definitions (10) were used previously [15, 19, 30] to model lead-acid batteries. The following numerical definitions were used to complete the model: R_{bs}=0.0013 Ω, R_{b1}=2.84 Ω, R_{bp}=10e^3 Ω, C_{b1}=2.5 mF, C_{bp}=2*45*9*12*36000/ (125^2- 90^2) =4.650 KF.

3.5 MPPT of a Solar Electric Vehicle with Fuzzy Logic and P&O Controllers

3.5.1 MPPT of a Solar Vehicle with P&O Controller

The performance of our MPPT applied to a solar-powered vehicle is compared to one of the most conventionally used, a P&O MPPT algorithm [2, 20, 22, 26, 37]. The P&O algorithm used for comparison is illustrated in Figure 5. The P&O method works as follows: the system is perturbed by increasing or decreasing the array operating voltage and observing its impact on the output power as shown in Figure 5. V and I are measured to calculate the present array output power P(k). This value for P(k) is compared to the value obtained from the previous measurement P(k-1). If the output power has increased since the last measurement, the perturbation of the output voltage will continue in the same direction as in the last cycle. If the output power has decreased since the last measurement, the perturbation of the output voltage will be reversed in the opposite direction of the last cycle. The operating voltage V is perturbed with every MPPT cycle and as soon as the MPP is reached, V will oscillate around the ideal operating voltage V_{MPP}. These oscillations will result in a power loss which value depends on the step of a single perturbation. If the step width is large, the

MPPT algorithm will be responding quickly to sudden changes in operating conditions with the trade-off increased losses under stable or slowly changing conditions. If the step width is very small, the losses under stable or slowly changing conditions will be reduced, but the system will be only able to respond very slowly to rapid changes in temperature or irradiance.

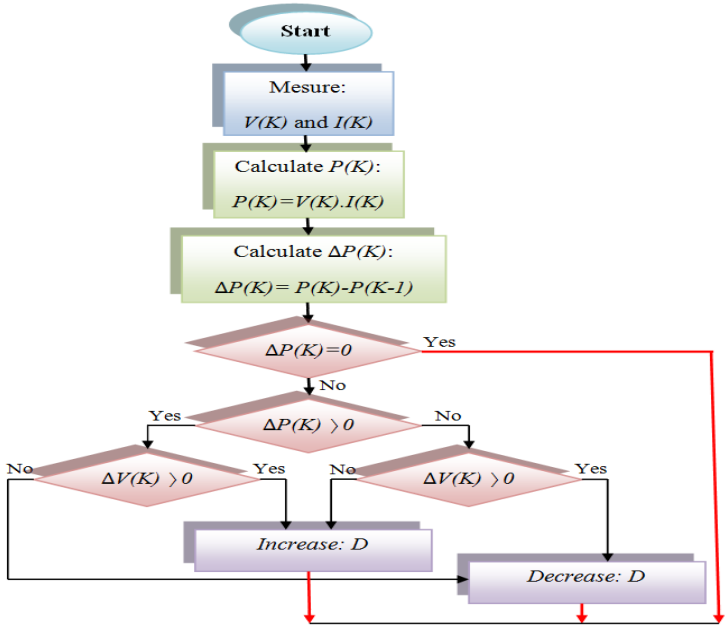

Figure 5
Flowchart of the P&O MPPT algorithm used for comparison

3.5.2 MPPT of a Solar Vehicle with Fuzzy Logic Controller

The Fuzzy Logic Control (FLC) is a rule-based algorithm which has the advantages of working with imprecise inputs, it does not need an accurate mathematical model and it can handle nonlinearity as well. Because of advantages like (1) Flexible operation, (2) Convenient user interface, (3) ease of implementation and (4) Qualified validation, the Fuzzy method is preferred in implementation for MPPT [38]. FLC constitutes four parts, which include fuzzification, inference, rule base, and defuzzification as shown in Figure 6.

In these parts, Fuzzy inference and designing of fuzzy rules decide the optimal performance of the system [41, 42]. But then, to design Fuzzy rules abundant knowledge and high amount of training is needed. The inputs to an MPPT fuzzy logic controller are usually an error E and a change in error ΔE. The user has the flexibility of choosing how to compute E and ΔE. Since dP/dV vanishes at the MPP.

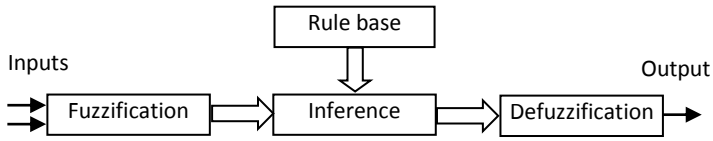

Figure 6
Block diagram of fuzzy logic controller

The common approaches made in FLC based MPPT are to reduce the error in the systems. In most of the cases, the error and difference in error are calculated based on the Equations (11) and (12).

$$E(K) = \frac{P(K) - P(K-1)}{I(K) - I(K-1)} \tag{11}$$

$$CE(K) = E(K) - E(K-1) \tag{12}$$

Where 'K' refers to iteration number, 'CE' is the change in error, 'E' is the error, 'P' is the power and 'I' is the current. Table 1 explaining the rules for determining the error and the change in error is given. In Fuzzy implemented MPPT, the variable duty cycle is considered for an effective tuning of a duty cycle [50, 51]. For instance, the error (E) and the change in error (CE) associated with the duty cycle is calculated. If the error value is PB (Positive Big) and the change in error value is PS (Positive Small), the rules are predefined in the lookup table.

Table 1
Fuzzy logic rule table/lookup table

E / CE	NB	NS	ZE	PS	PB
NB	ZE	ZE	PB	PB	PB
NS	ZE	ZE	PS	PS	PS
ZE	PS	ZE	ZE	ZE	NS
PS	NS	NS	NS	ZE	ZE
PB	NB	NB	NB	ZE	ZE

Decision on the duty 'ZE (zero)' has to be added with control variable for next cycle. Similar, the process is continued until the optimal location is reached. The key tool to choose fuzzy logic control is for its better accuracy, the ability to detect the error in quick time and tracking speed. The representation of membership function error 'E', change in error 'CE' and calculation of output variable duty variable 'D' is shown in Figure 7.

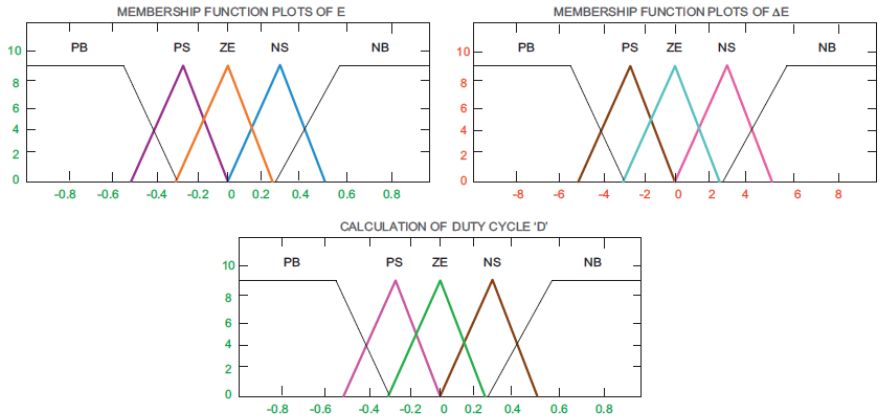

Figure 7

Membership function plots for E, ΔE, and calculation of duty cycle 'D'

The Fuzzy Logic based MPPT is based on the following algorithm:

1) The derivative of the P(V) function is used to locate the actual operation point P_i. Based on the result, the controller decides whether to increase or decrease the voltage, through the applied load to the duty ratio ΔD.

2) The second derivative of the P(V) function expresses the rate of approach or distancing of the point P_i from the MPP. These data are used by the controller for fast search of MPP. A fuzzy logic controller consists of three main operations: "fuzzification", "inference" and "defuzzification". The input sensory (crisp or numerical) data are fed into the fuzzy logic rule-based system where physical quantities are represented into linguistic variables with appropriate membership functions. These linguistic variables are then used in the antecedents (IF-Part) of a set of fuzzy "IF-THEN" rules within an inference engine to result in a new set of fuzzy linguistic variables or consequent (THEN-Part). During the fuzzification part, the controller instantaneously measures the voltage V(k) and current I(k) of a photovoltaic array and calculates output power as P(k)=I(k)V(k). The controller analyses $input_1(k)$, which expresses the slope of the current operating point on the P-V curve and $input_2(k)$: which expresses the rate of change of approach or distancing of the point p_i. The fuzzy logic controller takes instantaneous measurements of these two points then decides and calculates the output, ΔD(k) which is actually the change of the duty ratio of the MOSFET power switch. The input and output variables of the fuzzy logic controller must be expressed in terms of membership functions. Determination of the range of the fuzzy linguistic variables that compose the membership functions of input and output variables of the fuzzy logic controller is based on automation specialists experience, as described in the literature [39, 46].

Unlike commonly used FLC described previously, in this paper the FLC uses Gaussian form in membership functions. The Gaussian functions facilitate obtaining smooth, continuously differentiable hypersurfaces of a fuzzy model. They also facilitate theoretical analysis of fuzzy systems as they are continuously differentiable and infinitely differentiable, i.e. they have derivatives of any grade [47, 48, 49].

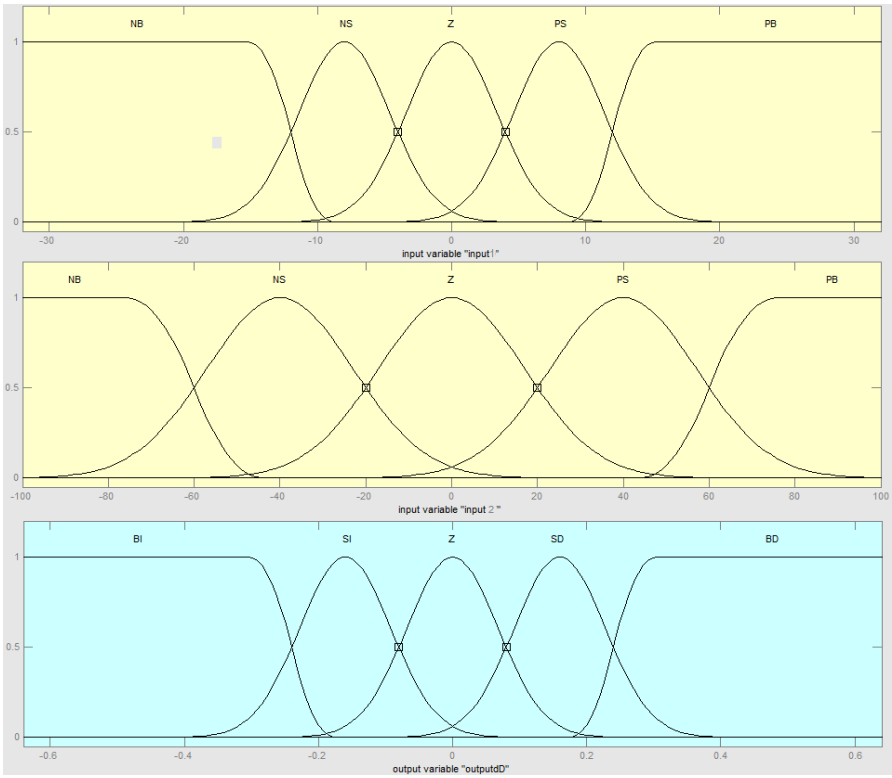

Figure 8

Membership functions of the two entries and the output: (a) Input1, (b) Input2 and (c) Output dD with five sets of linguistic Gaussian variables

The inputs and the outputs as sets of linguistics variables are expressed as follows:

Input1: NB: Negative Big, NS: Negative Small, Z: Zero, PB: Positive Big, PS: Positive Small.

Input2: NB: Negative Big, NS: Negative Small, Z: Zero, PB: Positive Big, PS: Positive Small.

Output: BD: Big Decrease, SD: Small Decrease, S: stabilize, BI: Big Increase, SI: Small Increase.

The value of $Input_1$, $Input_2$ and Output are normalized by an input scaling factor [4]. In this system the input scaling factor has been designed such that:

$Input_1$ values are between -32 and 32

$Input_2$ values are between -100 and 100

Output values are between -62 and 62

The inference method works in such a way that a change in the duty ratio of the buck chopper leads to the voltage V_{MPP} corresponding to the MPP. Following the study of an exhaustive number of combinations of input variables and analysis of the corresponding outputs, we came up with the decision inference rules illustrated in Figure 9.

1. If (input1 is NB) and (input2 is NB) then (outputdD is S) (1)
2. If (input1 is NS) and (input2 is NB) then (outputdD is S) (1)
3. If (input1 is Z) and (input2 is NB) then (outputdD is SD) (1)
4. If (input1 is PS) and (input2 is NB) then (outputdD is SI) (1)
5. If (input1 is PB) and (input2 is NB) then (outputdD is BI) (1)
6. If (input1 is NB) and (input2 is NS) then (outputdD is S) (1)
7. If (input1 is NS) and (input2 is NS) then (outputdD is S) (1)
8. If (input1 is Z) and (input2 is NS) then (outputdD is SI) (1)
9. If (input1 is PS) and (input2 is NS) then (outputdD is SI) (1)
10. If (input1 is PB) and (input2 is NS) then (outputdD is BI) (1)
11. If (input1 is NB) and (input2 is Z) then (outputdD is BD) (1)
12. If (input1 is NS) and (input2 is Z) then (outputdD is SD) (1)
13. If (input1 is Z) and (input2 is Z) then (outputdD is S) (1)
14. If (input1 is PS) and (input2 is Z) then (outputdD is SI) (1)
15. If (input1 is PB) and (input2 is Z) then (outputdD is BI) (1)
16. If (input1 is NB) and (input2 is PS) then (outputdD is BD) (1)
17. If (input1 is NS) and (input2 is PS) then (outputdD is SD) (1)
18. If (input1 is Z) and (input2 is PS) then (outputdD is S) (1)
19. If (input1 is PS) and (input2 is PS) then (outputdD is S) (1)
20. If (input1 is PB) and (input2 is PS) then (outputdD is S) (1)
21. If (input1 is NB) and (input2 is PB) then (outputdD is BD) (1)
22. If (input1 is NS) and (input2 is PB) then (outputdD is SD) (1)
23. If (input1 is Z) and (input2 is PB) then (outputdD is SI) (1)
24. If (input1 is PS) and (input2 is PB) then (outputdD is S) (1)
25. If (input1 is PB) and (input2 is PB) then (outputdD is S) (1)

Figure 9
Proposed Fuzzy Rules decisions

In this work, the Mamdani fuzzy inference method has been used with Max-Min operation fuzzy composition law. This method allows the definition of minimum and maximum input impact for all operating scenarios as illustrated in Figure 10.

Following "inference" operation, the controller outputs expressed as a linguistic variable curve. "Defuzzification" methods are then used to calculate and decode the linguistic variable to a numerical value. In this work, we make use of a Centroid Method, which determines the crisp controller Output as the value of the center of gravity of the final combined fuzzy set.

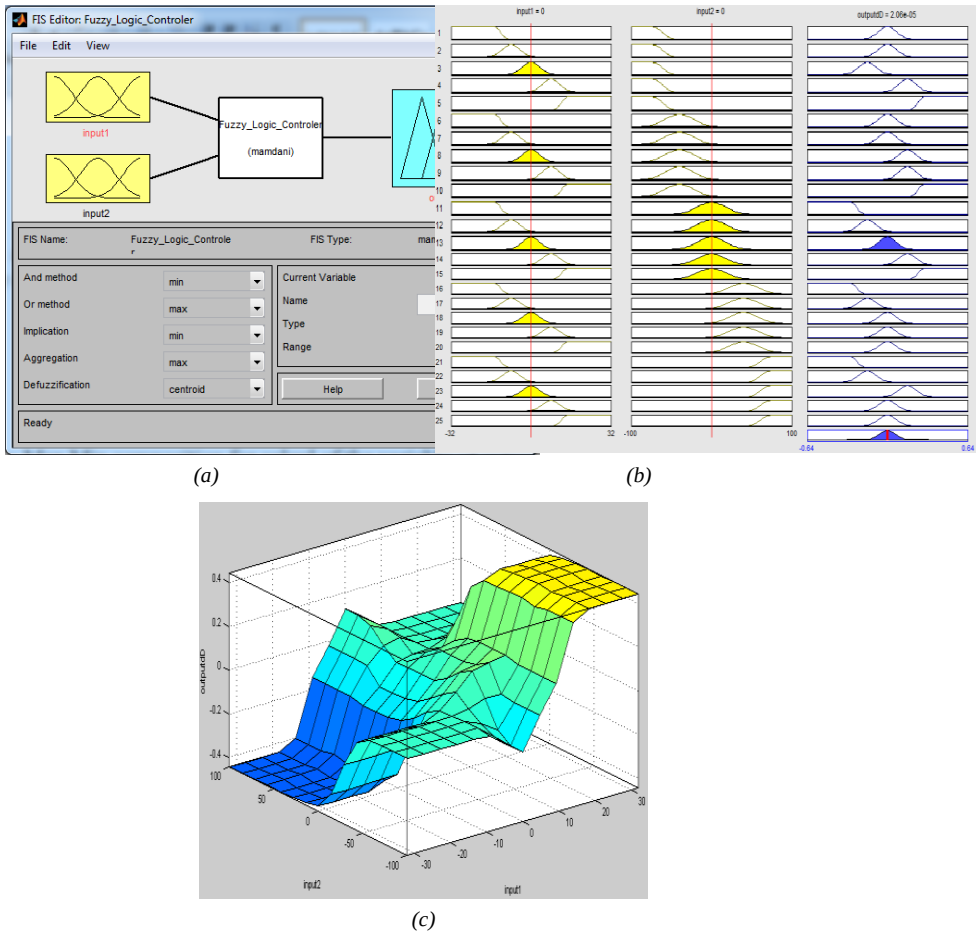

Figure 10
a) MATLAB representation of the Mamdani fuzzy logic controller; b) Output values depending on possible combinations of Input variables; c) Surface representation used for computation of the Output variable ΔD (center of gravity)

4 Simulation Model

The mathematical representation of the PV-powered section of the electric vehicle expressed through equations (1-4) with specific parametric definition given as follows: 5 series of connected solar panels consisting of 56 photovoltaic cells in series such that referring to Figure 2: z=56, R_p=30 Ω, R_s=15.10^{-3} Ω, E_g=1.1 eV, n_1=1; n_2=2, k=1.380 ×10^{-23} J/K, q=1.602×10^{-19} C, $I_{ph}\big|_{(T=298\cdot K)} = 3.25A$.

The buck converter is modeled by equations (5-8) with specific parametric values: $C_1 = C_2 = 5.6$ mF, L= 3.5 mH.

The solar car load block lead acid battery has been modeled by equations (9–10) with initial output voltage V_b=95 V and the following numerical definitions: R_{bs}= 0.0013 Ω, R_{b1}= 2.84 Ω, R_{bp}=10e^3 Ω, C_{b1}=2.5 mF, C_{bp}=2*45*9*12*36000/ (125^2-90^2) =4.650 KF.

The initial output of the MPPT was set to d=0.1(fuzzy logic), d=0.5(P&O).

The initial input of the MPPT was set to P=0 W and V=0V (fuzzy logic), P=0W and V=0V (P&O).

The parameters described above were integrated into the Simulink blocks shown in Figure 9 and Figure 10

Figure 9 describes the PV system implementing the P&O algorithm using Model-Based Design in order to control the Buck converter, and harvest the maximum power.

In Figure 11 the same blocks are maintained whereas the block of P&O was replaced by fuzzy logic Block.

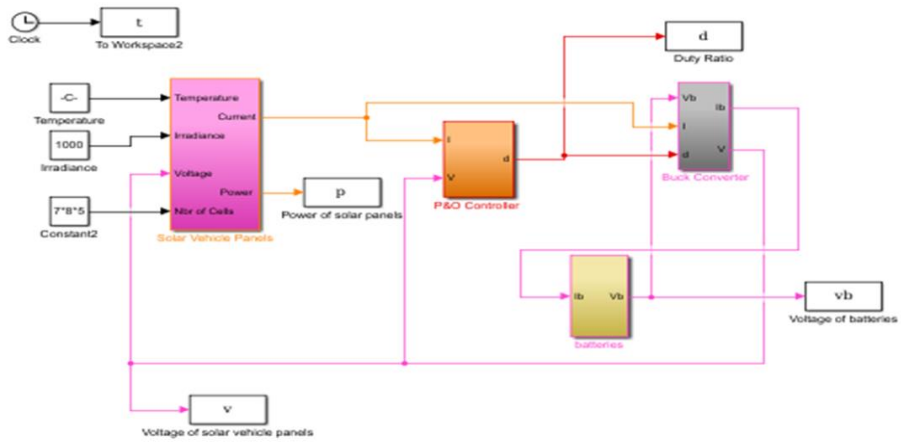

Figure 11
Solar vehicle PV system simulated in Matlab/Simulink with P&O controller

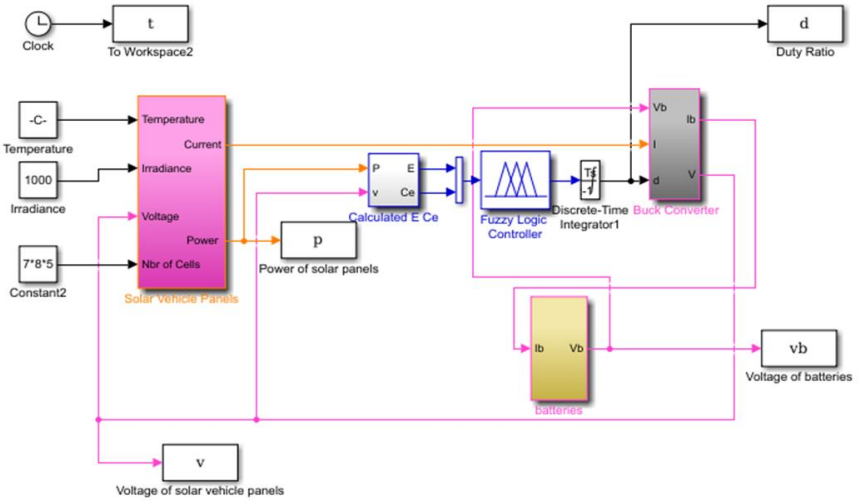

Figure 12

Solar vehicle PV system simulated in Matlab/Simulink with a fuzzy logic controller

5 Simulation Results

In an attempt to evaluate the performance improvement of a fuzzy logic based MPPT applied to a solar vehicle system, we analyzed its power extraction capabilities and stability versus the traditional P&O controller. In this simulation, the model of a solar vehicle was run with a fuzzy logic controller and a P&O controller under different climatic conditions, relevant to the movement of a solar vehicle, i.e., with rapid changes of irradiance and temperature.

5.1 Simulation Results for a Fast Increase of Irradiance

The first performance comparison between the fuzzy controller and conventional P&O controller was for a fixed temperature of 25ºC and a virtually instantaneous increase of irradiance from 100 Wm^{-2} to 1100 Wm^{-2} that occurs at t=25 s (Figure 13).

As expected, we note that with the rapid irradiance increase, the harnessed power also increased. In the case of the P&O controller, we note that there is a very harsh overshoot of the power signal. The power signal for the P&O controller rapidly increases and then abruptly drops to increase progressively to a seemingly steady state of maximum power. However, when zoomed in, we note that the P&O controller generated signal actually oscillates about a mean and is not stable. Similar overshoots are obtained for operating voltages for solar panels and solar batteries in the case of the P&O controller. This leads, not only to reduce energy

being harvested but also to cyclic recurrent electric changes on the elements with possible lifecycle reduction. We note a much better performance of the fuzzy logic based controller. First of all, in the case of all signals (voltage and power), the steady state signal is very stable. Furthermore, we note that the response time to detect MPP and achieve maximum power harvest is shorter compared to the P&O controller with limited overshoot.

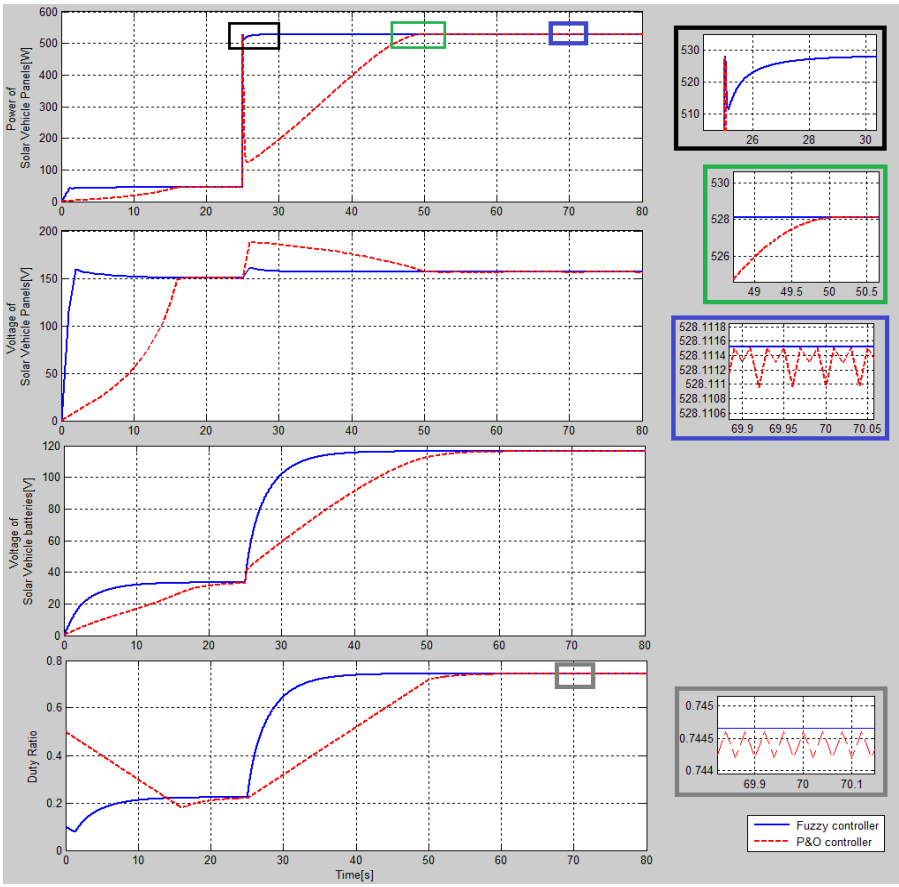

Figure 13

Performance comparison between P&O and a fuzzy logic controllers for an instantaneous increase of irradiance from 100 Wm^{-2} to 1100 Wm^{-2} at t=25 s for fixed temperature of 25ºC

5.2 Simulation Results for a Fast Decrease of Irradiance

In this case, we compare the relative performance of fuzzy logic controller with a conventional P&O controller for a fixed temperature of 25ºC and a virtually instantaneous decrease of irradiance from 1000 Wm^{-2} to 400 Wm^{-2} at t=25 s (Figure 14).

Similar advantages are noticed for the fuzzy logic controller with shorter time response for maximum power point identification and power stabilization. However, the performance disparity between the two controllers is less than the previous case of the rapid increase in irradiance. In this case, the major advantage of the fuzzy logic controller is during the steady-state operation with an increase of power and voltage stability and overshoot reduction.

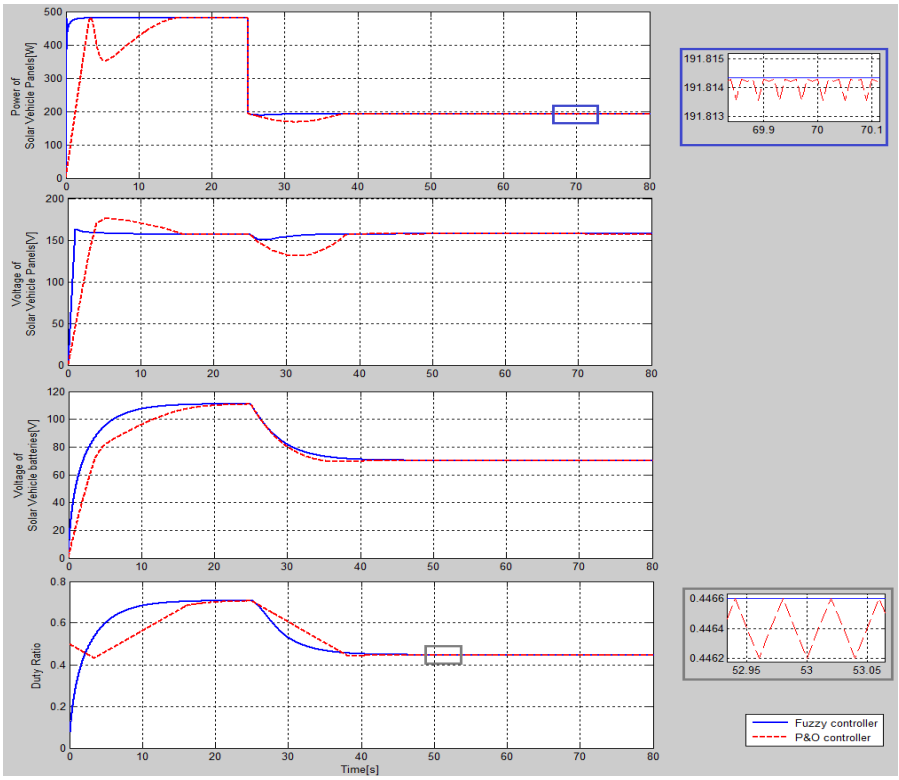

Figure 14

Performance comparison between P&O and a fuzzy logic controller for an instantaneous decrease of irradiance from 1000 Wm^{-2} to 400 Wm^{-2} at t=25 s for a fixed temperature of 25°C

5.3 Simulation Results for a Fast Increase in Temperature

Because of the influence of the temperature, which acts negatively on the efficiency of photovoltaic systems, it is essential to study the behavior of the two controllers for abrupt variations of temperature. The two controllers FL and P&O will be subject to an instantaneous increase of temperature from 10°C to 50°C at a fixed irradiance of 1000 Wm^{-2} (Figure 15).

The performances of FL controller are definitely more appreciable with a better response time and overshoot reduction and less oscillation in steady state.

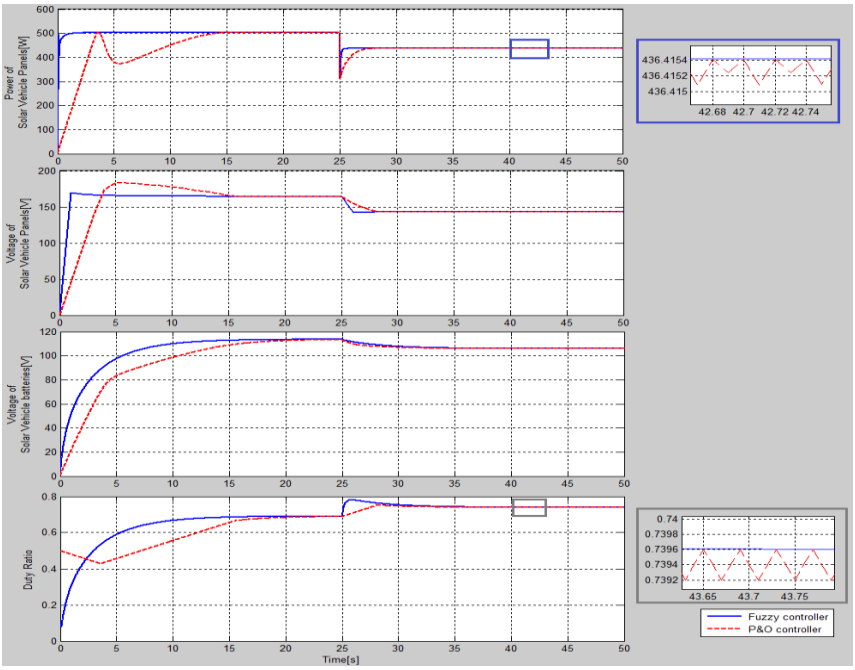

Figure 15

Performance comparison between P&O and a fuzzy logic controller for an instantaneous increase of temperature from 10ºC to 50ºC (at t=25 s) at a fixed irradiance of 1000 Wm^{-2}

5.4 Simulation Results for a Fast Decrease in Temperature

In a second test, where the temperature falls abruptly from 60°C to 05°C with a fixed irradiance of 1000 Wm^{-2}, the same performances described above are noticed with a better time of response, a limited overshoot and reduced oscillations in the steady state. This state represents a precious gain of time and energy for the vehicle that changes position all the time of which sudden changes in irradiance and temperature are always expected (Figure 16).

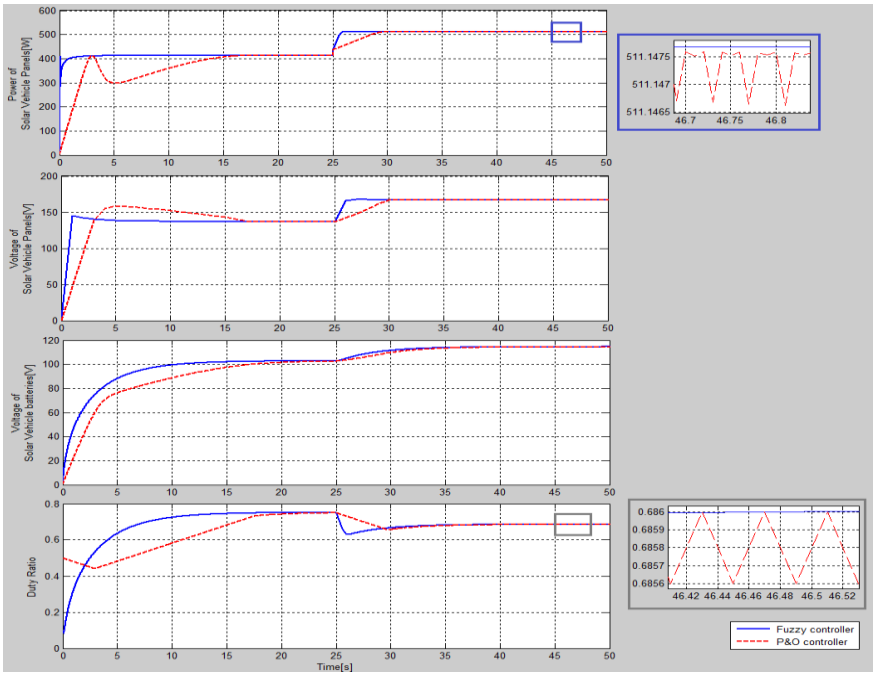

Figure 16

Performance comparison between P&O and a fuzzy logic controller for an instantaneous decrease of temperature from 60ºC to 5ºC (at t=25 s) at a fixed irradiance of 1000 Wm^{-2}

Conclusion

The initial cost of solar energy is a major issue in relation to its huge potential for greater development. Maximum power extraction is an important parameter to reduce the total cost of PV systems and enables better paybacks of PV projects. In this paper, we focused our analysis on solar-powered vehicles. A rapidly adapting MPP algorithm is required to harness the maximum power and make such applications technologically and cost effective. We proposed a new fuzzy logic method to achieve a faster and more stable power output from PV modules. In order to emphasize the performance of this new controller, a Matlab-Simulink® model was built and simulations were run for various operational scenarios. The results were compared with a commonly used P&O controller. Simulation results prove a high efficiency, in maximum power tracking, of a fuzzy logic controller. The simulations showed that most significant performance differences were achieved with rapidly varying parameters that influence power output (temperature and irradiance). Moreover, the fuzzy logic-based controller, as compared to the P&O controller, shows better performance in maximum power tracking time, and stability and robustness in all cases. Better stability and a robust performance from the fuzzy logic based controller, offers significant advantages in the mitigation of power fluctuations.

Acknowledgment

The authors would like to thank Dr. Khaled Ragab (UQAC University, Chicoutimi, QC, Canada) for his efforts in revising the academic written English of this article.

References

[1] Cheddadi, Y., et al: Design and verification of photovoltaic MPPT algorithm as an automotive-based embedded software. Solar Energy 171: 414-425. 2018

[2] Karami, N., et al: General review and classification of different MPPT Techniques." Renewable and Sustainable Energy Reviews 68: 1-18. 2017

[3] Makhsoos, A., et al: Design, simulation and experimental evaluation of energy system for an unmanned surface vehicle." Energy 148: 362-372. 2018

[4] Yilmaz, U., et al: PV system fuzzy logic MPPT method and PI control as a charge controller." Renewable and Sustainable Energy Reviews 81: 994-1001 (2018)

[5] Anurag, A., et al: A review of maximum power-point tracking techniques for photovoltaic systems. International Journal of Sustainable Energy, 2016. **35**(5): pp. 478-501

[6] Shweta Pandey, Prasanta Kumar Jena: A Review on Maximum Power Point Tracking Techniques for Photovoltaic Systems. International Research Journal of Engineering and Technology (IRJET). Volume: 04 Issue: 06 | June -2017

[7] Onat, N: Recent developments in maximum power point tracking technologies for photovoltaic systems. International Journal of Photoenergy, 2010

[8] M. Oulcaid, H. El Fadil, A. Yahya, F. Giri: Maximum Power Point Tracking Algorithm for Photovoltaic Systems under Partial Shaded Conditions. IFAC-PapersOnLine. Vol. 49, Issue 13, 2016, pp. 217-222

[9] Won, C.-Y., et al: A new maximum power point tracker of photovoltaic arrays using fuzzy controller. In Power Electronics Specialists Conference, PESC'94 Record. 25th Annual IEEE. 1994. IEEE

[10] Ahmed M. Othman, Mahdi M. M. El-arini, Ahmed Ghitas, Ahmed Fathy: Realworld maximum power point tracking simulation of PV system based on Fuzzy Logic control. Volume 1, Issue 2, December 2012, pp. 186-194

[11] Patcharaprakiti, N., S. Premrudeepreechacharn, and Y. Sriuthaisiriwong: Maximum power point tracking using adaptive fuzzy logic control for grid-connected photovoltaic system. Renewable Energy, 2005. **30**(11): pp. 1771-1788

[12] Juntao Fei, Yunkai Zhu: Adaptive fuzzy sliding control of single-phase PV grid-connected inverter. PLoS ONE 12(8): e0182916. https://doi.org/ 10.1371/journal.pone.0182916. August 10, 2017

[13] Subhash E. Apatekar, Akireddy Shravankumar, Ch. Anitha: Maximum Power Point Tracking using Fuzzy Logic Control for Grid-Connected Photovoltaic System & Operation of PV Cells under Partial Shading Conditions. International Conference on Recent Trends in Engineering Science and Technology (ICRTEST 2017) Volume 5, Issue 1 (Special Issue 21-22 January 2017)

[14] Cheikh, M. A., et al: Maximum power point tracking using a fuzzy logic control scheme. Revue des energies Renouvelables, 2007. **10**(3) pp. 387-395

[15] Sadeq D. Al-Majidi, Maysam F. Abbod, Hamed S. Al-Raweshidy: A novel maximum power point tracking technique based on fuzzy logic for photovoltaic systems. International Journal of Hydrogen Energy. Volume 43, Issue 31, 2 August 2018, pp. 14158-14171

[16] Salameh, Z. M., M. A. Casacca, and W. A. Lynch: A mathematical model for lead-acid batteries. IEEE Transactions on Energy Conversion, 1992. 7(1): pp. 93-98

[17] Leszek Kasprzyk: Modelling and analysis of dynamic states of the lead-acid batteries in electric vehicles. Eksploatacja i Niezawodnosc – Maintenance and Reliability 2017; 19 (2): 229-236

[18] Larbes, C., et al: Genetic algorithms optimized fuzzy logic control for the maximum power point tracking in photovoltaic system. Renewable Energy, 2009. **34**(10): pp. 2093-2100

[19] Mohamed Amine Haraoubia, Najib Essounbouli, Abdelaziz Hamzaoui: Optimisation of fuzzy controller for tracking the maximum power point in PV systems. IEEE 2015 3rd International Renewable and Sustainable Energy Conference (IRSEC)

[20] Khaligh, A. and O. C. Onar: Energy harvesting: solar, wind, and ocean energy conversion systems. 2017: CRC press

[21] Kamarzaman, N. A. and C. W. Tan: A comprehensive review of maximum power point tracking algorithms for photovoltaic systems. Renewable and Sustainable Energy Reviews, 2014. 37: pp. 585-598

[22] Jaldeep Kumar, Prakash Bahrani: Comprehensive Review on maximum power point tracking methods for SPV system. International Research Journal of Engineering and Technology (IRJET) Volume 04, Issue 12 | Dec-2017

[23] Esram, T. and P. L. Chapman: Comparison of photovoltaic array maximum power point tracking techniques. IEEE Transactions on energy conversion, 2007. 22(2): pp. 439-449

[24] Manel Hlaili and Hfaiedh Mechergui: Comparison of Different MPPT Algorithms with a Proposed One Using a Power Estimator for Grid Connected PV Systems. International Journal of Photoenergy. Volume 2016, Article ID 1728398, 10 pages

[25] Hua, C. and C. Shen: Comparative study of peak power tracking techniques for solar storage system. In Applied Power Electronics Conference and Exposition, 1998. APEC'98. Conference Proceedings 1998. Thirteenth Annual. 1998, IEEE

[26] Fernando Lessa Tofoli. Dênis de Castro Pereira. Wesley Josias De Paula: Comparative Study of Maximum Power Point Tracking Techniques for Photovoltaic System. in International Journal of Photoenergy 2015(3):1-10 February 2015

[27] Reisi, A. R., M. H. Moradi, and S. Jamasb: Classification and comparison of maximum power point tracking techniques for photovoltaic system: A review. Renewable and Sustainable Energy Reviews, 2013. 19: pp. 433-443

[28] Priety, Vijay Kumar Garg: A review paper on various types of MPPT techniques for PV system. International Journal of Engineering & Science Research. IJESR/May 2014/ Vol-4/Issue-5/320-330

[29] Knopf, H: Analysis, simulation, and evaluation of maximum power point tracking (MPPT) methods for a solar powered vehicle. 1999, Portland State University Portland

[30] Athanasios G. Sarigiannidis, Spyridon A. Stathis, Antonios G. Kladas: Performance evaluation of MPPT techniques for PV array incorporated into Electric Vehicle roof. IEEE, 2015 International Conference on Renewable Energy Research and Applications (ICRERA)

[31] Swokowski, E. W: Analyse. 1993: De Boeck Supérieur

[32] Wolfs, P. and Q. Li: A current-sensor-free incremental conductance single cell MPPT for high performance vehicle solar arrays. in *Power Electronics Specialists Conference, 2006. PESC'06. 37th IEEE*. 2006. IEEE

[33] Sheifali Gupta. Ankit Aneja. Hitesh Mittal. Aditya Jai: Performance and Cost Optimised MPPT for Solar Powered Vehicle. International Journal of Advanced Research in Computer Engineering & Technology (IJARCET) Volume 2, Issue 12, December 2013

[34] Yuli, H. and W. Jiajun: Study on power generation and energy storage system of a Solar Powered Autonomous Underwater Vehicle (SAUV) Energy Procedia, 2012. 16: pp. 2049-2053

[35] Ali Razmjoo, Mohammad Ghadimi, Mehrzad Shams, Hoseyn Shirmohammadi: Design and Built a Research AUV Solar Light Weight. International Journal of Energy and Power Engineering. 2015; 4(5) 268-274

[36] Skaale, I., D. J. Patterson, and H. Pullen: The development of a new maximum power point tracker for a very high efficiency, compound curve photovoltaic array for a solar powered vehicle. Renewable Energy, 2001. 22(1-3): pp. 295-302

[37] K. Someswara Rao, V. Mahesh, Jammula. Kalyan Chakravarthi, Syed Khutub Uddin: Design and Development of Green Car. ISSN (Print): 2319-3182, Volume 3, Issue 4, 2014

[38] Ram, J. P., et al: A comprehensive review on solar PV maximum power point tracking techniques. Renewable and Sustainable Energy Reviews 67: 826-847, 2017

[39] Amitava Chatterjee. Ranajit Chatterjee. Fumitoshi Matsuno. Takahiro Endo: Augmented Stable Fuzzy Control for Flexible Robotic Arm Using LMI Approach and Neuro-Fuzzy State Space Modeling. in IEEE Transactions on Industrial Electronics 55(3):1256 -1270, April 2008

[40] Tamás Haidegger, Levente Kovács, Radu-Emil Precup, Balázs Benyó, Zoltán Benyó, Stefan Preitl: Simulation and control for telerobots in space medicine. Acta Astronautica, Vol. 81, Issue 1, December 2012, pp. 390-402

[41] Petr HušEk, Otto Cerman: Fuzzy model reference control with adaptation of input fuzzy sets. Knowledge-based Systems. Volume 49, September, 2013, pp. 116-122

[42] Sasa Vrkalovic, Teodor-Adrian Teban, Ioan-Daniel Borlea: Stable Takagi-Sugeno Fuzzy Control Designed by Optimization. Control Designed by Optimization, International Journal of Artificial Intelligence, Vol. 15, No. 2, pp. 17-29, 2017

[43] Ko, S.-H. and R.-M. Chao: Photovoltaic dynamic MPPT on a moving vehicle. Solar Energy, 2012. **86**(6): pp. 1750-1760

[44] Ismail Nakir. Ali Durusu. Hakan Akca. Ali Ajder: A New MPPT Algorithm for Vehicle Integrated Solar Energy System. in Journal of Energy Resources Technology 138(2) November 2015

[45] Salameh, Z. and D. Taylor: "Step-up maximum power point tracker for photovoltaic arrays". Solar energy, 1990. **44**(1): pp. 57-61

[46] Casacca, M. A. and Z. M. Salameh: Determination of lead-acid battery capacity via mathematical modeling techniques. IEEE Transactions on Energy Conversion, 1992, 7(3): pp. 442-446

[47] Ahsanullah Soomro, Wenguo Xiang, Kamran A Samo: Development of a simplified method for the determination of ampere-hour capacity of lead–acid battery. Energy & Environment, November 28, 2017

[48] Lu, C.-F., C.-C. Liu, and C.-J. Wu: Dynamic modelling of battery energy storage system and application to power system stability. IEEE Proceedings-Generation, Transmission and Distribution, 1995, **142**(4): pp. 429-435

[49] Xiaokang Xu, Martin Bishop, Donna G. Oikarinen, Chen Hao: Application and modeling of battery energy storage in power systems. CSEE Journal of Power and Energy Systems (Volume 2, Issue 3, Sept. 2016)

[50] Bühler, H: *Réglage par logique floue*. 1994: Presses polytechniques et universitaires romandes

[51] Piegat, A: (2013) Fuzzy modeling and control, Physica